

# Competing interactions in two dimensional Coulomb systems: Surface charge heterogeneities in coassembled cationic-anionic incompatible mixtures

Sharon M. Loverde, Yury S. Velichko, and Monica Olvera de la Cruz<sup>a)</sup>

*Department of Materials Science and Engineering, Northwestern University, Evanston, Illinois 60208-3108*

(Received 13 January 2006; accepted 8 February 2006; published online 11 April 2006)

A binary mixture of oppositely charged components confined to a plane such as cationic and anionic lipid bilayers may exhibit local segregation. The relative strengths of the net short range interactions, which favors macroscopic segregation, and the long range electrostatic interactions, which favors mixing, determine the length scale of the finite size or microphase segregation. The free energy of the system can be examined analytically in two separate regimes, when considering small density fluctuations at high temperatures and when considering the periodic ordering of the system at low temperatures [F. J. Solis, S. I. Stupp, and M. Olvera de la Cruz, *J. Chem. Phys.* **122**, 054905 (2005)]. A simple molecular dynamics simulation of oppositely charged monomers, interacting with a short range Lennard-Jones potential and confined to a two dimensional plane, is examined at different strengths of short and long range interactions. The system exhibits well-defined domains that can be characterized by their periodic length scale as well as the orientational ordering of their interfaces. By adding salt, the ordering of the domains disappears and the mixture macroscopically phase segregates in agreement with analytical predictions. © 2006 American Institute of Physics. [DOI: [10.1063/1.2181573](https://doi.org/10.1063/1.2181573)]

## I. INTRODUCTION

Biological and synthetic heterogeneous charged molecules are expected to self-organize in aqueous solutions into complex ionic structures. Coassemblies of oppositely charged molecules are ubiquitous, given that nucleic acids and most proteins are charged. The structure of oppositely charged bimolecular coassemblies, such as DNA proteins in nucleosomes<sup>1</sup> and actin-protein complexes in the cytoskeleton,<sup>2</sup> is the result of the competition of short range interactions, including excluded volume, and electrostatics. Cationic and anionic mixtures of lipids or peptide amphiphiles coassembled into vesicles<sup>3,4</sup> or cylindrical micelles<sup>5-7</sup> are examples of coassemblies stabilized by hydrophobic interactions and electrostatics. The surfaces of such complexes of oppositely charged molecules may not be homogenous if the chemically coassembled structures have net repulsive short range interactions among them or if the charges exposed to the surfaces have different degrees of compatibilities with water. Understanding the surface assembly of a complex group of charged components may lead to a greater deal of understanding concerning the stability of self-assembled aggregates. Moreover, it may give insight into the complex behavior of lipid rafts and their contribution towards protein sorting and cell signaling.<sup>8</sup>

Bulk solution properties of electrostatic driven coassemblies of cationic and anionic macroions have been extensively studied. Examples of these are the DNA in cationic molecules of valence 3+ and higher,<sup>9,10</sup> as well as other synthetic strongly charged polyelectrolytes in metallic multiva-

lent salts.<sup>11</sup> These hydrated multivalent ions are known to induce the precipitation of strongly charged chains of opposite charges into dense ionic structures.<sup>12-14</sup> Coassemblies of hydrophobic molecules of opposite charges, however, are less understood. Surface heterogeneities in coassembled chemically incompatible oppositely charged molecules have been recently predicted analytically.<sup>14</sup> The surface charge heterogeneities are due to the competition between the long range electrostatic interactions (which decay as  $1/r$  because the surface is embedded in a three dimensional medium) and the short range interactions. The net incompatibility among the chemically different components of opposite charges promotes macroscopic segregation. Electrostatic interactions, on the other hand, promotes mixing into an ionic crystal structure. Consider cationic molecules with strong attractions among themselves and restricted to surfaces such as cationic lipids adsorbed onto the surface of mica, which is negatively charged.<sup>15,16</sup> The cationic molecules will aggregate into positively charged domains due to the strong net van der Waals attraction among them. The size of the domain, however, cannot grow past a characteristic size due to the high energetic penalty associated with the creation of a charged domain. This results in ordered finite size domains on the surface at low temperatures.<sup>17</sup> Finite size charged heterogeneities have been observed experimentally on charged surfaces in the presence of adsorbed self-aggregating molecules of opposite charges.<sup>2,16</sup> Moreover, lattice Monte Carlo simulations of incompatible cationic and anionic molecules restricted to the surface of cylinders reveal many interesting finite temperature effects as well as various stripe structures along the cylinder at lower temperatures.<sup>18</sup>

The formation of charged domains on a flat square lattice

<sup>a)</sup>Electronic mail: m-olvera@northwestern.edu

due to the competition between Coulomb interactions and net short range repulsion amongst oppositely charged molecules has been explored by simulation at zero temperature<sup>19</sup> and also by mean field arguments at high temperatures.<sup>18,19</sup> These stoichiometric mixtures develop ordered striped domains possessing a characteristic width that depends on the strength of the competing Coulomb and short range interactions at low temperatures. At high temperatures percolated structures develop, resembling a spinodal decomposition pattern during phase segregation of binary systems, but the growth is restricted, as in block copolymer systems with microphase segregation.<sup>20,21</sup> Here, we analyze the formation of the charged domains in two dimensions via molecular dynamics simulations at different ratios of the short and long range interactions. We analyze the symmetric case of equal head sizes of stoichiometric mixtures of +1 and -1 charges with different effective interactions among them. Finite temperature effects are discussed. In Sec. II analytic arguments are given for the scaling of the surface charge domain size in various regimes of the degree of incompatibility. We justify the existence of charged domains in surfaces, as compared to a bulk three dimensional system. In Sec. III we describe our simulations. In Sec. IV we discuss the results, and in the last section we give the conclusions.

## II. THEORY

The phase behavior of the ionic mixture can be examined in a simplistic manner analytically in two separate regimes. At higher temperatures, we consider small density fluctuations around the mean. At low temperatures, when the system exhibits strongly segregated domains, we assume that the system is periodic. At low temperature values, or high values of the magnitude of short range attraction, the system exhibits well-defined periodic lamellar when the surface charge coverage of the positive and negative molecules are equal and confined to a flat surface. The free energy of the system is dominated by the electrostatic cohesive energy, in addition to the interfacial contribution to the free energy, which is characterized by the line tension  $\gamma$  per thermal energy  $k_B T$ . Within the strong segregation regime, the entropic contribution to the free energy is negligible.

Following the example of the free energy for an incompressible two dimensional system of a mixture of positive and negative components,<sup>17</sup> we generalize the results for a course grained free energy scaling analysis for a  $d$  dimensional system of  $N_A$  positively and  $N_B$  negatively charged components interacting with a three dimensional Coulombic  $1/r$  potential. The free energy can be written as a sum of the total electrostatic interactions and the contribution from the line tension of each periodic segregated domain. Each charged domain is approximated by an electroneutral unit cell which has a characteristic lattice length  $L$ , dimensions  $L^d$ , and an associated charge density  $\sigma$ . The net free energy per total number of particles  $N=N_A+N_B$ , in units of  $k_B T$ , can be written as

$$\frac{F_{\text{NET}}}{N} = \frac{F_{\text{cell}}}{N_{\text{cell}}} \approx \frac{\alpha^d}{L^d} \left( \gamma s_1 L^{d-1} + \frac{l_B \sigma^2 s_2 (L^d)^2}{L} \right) = \left( \frac{F_0 \alpha^d}{L_0^d} \right) F. \quad (1)$$

Here,  $s_1$  and  $s_2$  are geometrical parameters that depend on the characteristic geometry of the underlying unit cell,  $\alpha^d$  represents the size of the particle, and  $N_{\text{cell}}$  represents the number of particles per unit cell. The Bjerrum length  $l_B$  is given by

$$l_B = \frac{e^2}{4\pi\epsilon\epsilon_0 k_B T}. \quad (2)$$

$F_0$  and  $L_0$  are system dependent parameters, defined by the minimization of the free energy of the system with respect to the characteristic size of the system,  $L$ ,

$$F_0 = \left( \frac{\gamma^{2d-1}}{(l_B \sigma^2)^{d-1}} \right)^{1/d} \quad (3)$$

and

$$L_0 = \left( \frac{\gamma}{l_B \sigma^2} \right)^{1/d}. \quad (4)$$

The dimensionless free energy per unit area in terms of  $s_1$  and  $s_2$  is then described by

$$F = \frac{s_1}{D} + s_2 D^{d-1}, \quad (5)$$

where  $D=L/L_0$  is the ratio of the characteristic size of the unit lattice to the length of the system. Minimizing the dimensionless free energy with respect to  $D$  gives the free energy of the favored periodic structure as

$$F = 2((d-1)s_2 s_1^{d-1})^{1/d}, \quad (6)$$

where

$$D = \left( \frac{s_1}{(d-1)s_2} \right)^{1/d}. \quad (7)$$

Depending on the area fraction of charge coverage,  $f$ , and the geometry of the unit lattice cell, the free energy can be calculated for different sets of crystalline structures. For an ideally symmetric system, consisting of equal components of positively and negatively charged molecules with similar head group sizes,  $f$  is 1/2. The minimum free energy in this case, for a two dimensional system, is characterized by lamellar structures.

We consider a line tension that is proportional to the immiscibility of the component molecules,  $\chi$ .<sup>22</sup> The Flory-Huggins parameter  $\chi$  is defined as the difference in the magnitudes of the short range interactions between two components,  $\chi = (\epsilon_{12} - \frac{1}{2}(\epsilon_{11} + \epsilon_{22})) / k_B T$ , where  $\epsilon_{ij}$  represents the pair interaction energy between  $i$  and  $j$ . For a lower or two dimensional system,  $L_0$  would be comparably larger than for a three dimensional system due not only to the  $1/d$  power law dependence but also to the decreased value of the Bjerrum length  $l_B$  for a surface in contact with water. For a surface in contact with an aqueous solution the mean permittivity of the medium is much higher than in a dense three dimensional system, which decreases the Bjerrum length  $l_B$ , and thus the

magnitude of  $L_0$ , significantly. For these reasons, patterning on a surface due to the competition of electrostatic interactions with short range interactions is considerably more feasible than the creation of charged domains in a bulk three dimensional system.

Comparing length scales with experimental systems, consider a two dimensional system of a single layer of positively and negatively charged lipids at an interface between water and an alternate medium. The average dielectric permittivity at the interface  $\epsilon_i \sim 40$ , in between that of the water  $\epsilon_{\text{water}} \sim 80$ , and that of the dense medium  $\epsilon_{\text{medium}} \sim 1$ . This would correspond to a Bjerrum length  $l_B \sim 2$  nm in terms of the a classical electrostatic interaction between charged head groups of the lipids exposed to the aqueous interface. Considering a large magnitude of the net interaction between tails of interacting lipids at the interface ( $\chi \sim 15$ ), depending on the length of the hydrophobic tail of the molecules ( $\sim 20$  carbons) and the charge density of the head group ( $\sim 0.6/\text{nm}^2$ ), this could correspond to a fairly large equilibrium domain size  $L_0$  ( $\sim 80$  nm). Domains of this size or larger have been seen for experimental systems of competing short range and long range electrostatic interactions, although in comparing with these systems, a variety of kinetic and specific interaction effects should also be considered.<sup>23,24</sup>

Next, consider the opposite, high temperature regime. Since the system does not exhibit well-defined periodic structures, the entropic contribution to the free energy cannot be ignored. In this case, the linear response theory or the random phase approximation for a compressible binary systems<sup>25</sup> is used to describe the behavior of the correlations as a function of the relative strength of the short range attraction and the electrostatic interactions. The random phase approximation involves an expansion of the free energy of the system in terms of density fluctuations, neglecting all terms larger than second order. For a general system of  $N$  components, where  $i$  and  $j$  represent components of a different type, the partition function can be written as<sup>11,26</sup>

$$Z = \frac{1}{N_A!N_B!} \int \exp\left(-\frac{H(r_i^{(1)}r_j^{(2)})}{k_B T}\right) \prod_i dr_i^{(1)} \prod_j dr_j^{(2)}, \quad (8)$$

where the Hamiltonian of the system is represented by

$$H(r_i^{(1)}r_j^{(2)}) = \sum_i \sum_j v_{ij}(r_i^{(1)} - r_j^{(2)}). \quad (9)$$

It is assumed that the interparticle potential can be broken up into a short range and a long range electrostatic potential,  $v_{ij} = v_{ij}^{\text{SR}} + v_{ij}^{\text{el}}$ . The short range contribution is assumed to be of the form of the Fourier transform of a Gaussian potential, which has been shown to reasonably predict thermodynamic properties of binary systems,<sup>27</sup>

$$v_{ij}^{\text{SB}}(r) = \frac{\epsilon_{ij}}{\pi a^2} e^{-r^2/a^2}. \quad (10)$$

The long range potential is represented by the Debye-Hückel potential,

$$v_{ij}^{\text{el}}(r) = \frac{z_i z_j l_B e^{-\kappa r}}{r}, \quad (11)$$

where  $\kappa$ , the inverse screening length, is defined by the concentration of salt in the solution. We assume that the density is a smooth function and can be represented by the sum of its Fourier components

$$\rho^i(r) = \sum_k \rho_k^i e^{ikr}. \quad (12)$$

In this case, the partition function becomes

$$Z = Z_0 \frac{A^{N_A} A^{N_B}}{N_A! N_B!} \int \exp\left(-\frac{1}{2A} \sum_{k \neq 0} \sum_{ij} (\mathbf{U}_k^{ij} + \rho_i^{-1} \delta_{ij}) \rho_k^i \rho_{-k}^j\right) \prod_{k>0} \prod_i \frac{d\rho_k^i}{\pi V \rho_i}, \quad (13)$$

where  $A$  represents the area of a two dimensional plane in a three dimensional volume  $V$ .  $Z_0$  includes the  $k$  zero and the self-energy terms.  $\mathbf{U}_k^{ij}$  is the sum of the interaction energies of the system, consisting of the short range interactions due to the excluded volume and hydrophobic interactions,  $v_{ij}^{\text{SR}}(k)$ , as well as the long range electrostatic potential  $v_{ij}^{\text{el}}(k)$ .

For an incompressible system of  $i$  same-sized components,

$$\sum_i \rho_k^i = 0. \quad (14)$$

For the case of an incompressible, neutral, symmetric system we also assume that  $\rho_+(k) = -\rho_-(k)$ . The electrostatic potential is the two dimensional Fourier transform of the screened Coulomb interaction between charge density fluctuations,

$$U_{\text{el}}(k) = \int d^2 r e^{ikr} \frac{\sigma z_T^2 l_B e^{-\kappa r}}{r} = \frac{1}{2} \sigma z_T^2 \frac{2\pi l_B}{\sqrt{\kappa^2 + k^2}}, \quad (15)$$

where  $\sigma$  represents the charge density of the system and  $z_T$  represents the total positive and negative charges of the components. In this case, the inverse structure factor has the following contributions:

$$\frac{1}{S_0(k)} = U_k + \rho^{-1} = \frac{1}{\rho} + \frac{1}{1-\rho} - 2\chi + \chi k^2 + U_{\text{el}}(k). \quad (16)$$

The structure function has a peak at the most probable wavelengths,  $k^*$ . For the case when there is no screening the location of the peak  $k^*$  scales with the Bjerrum length  $l_B$  and the magnitude of the short range attraction,  $\epsilon$ , as  $k^* \sim (\epsilon/l_B)^{1/(d+1)}$ . The scaling of the periodic order of the system changes at the transition temperature from  $-(1+d)$  at higher temperatures considering small density fluctuations to  $-d$  at lower temperatures [Eq. (4)], which is predicted using the previously described theory of strong segregation. For a two dimensional system, which is the subject of interest, the scaling is predicted to change from  $-1/3$  to  $-1/2$  as the temperature decreases.

At high temperatures, in the nearly isotropic state, the total free energy of the system per unit volume, in units of  $k_B T$ , can be written as

TABLE I. Interspecies potentials.

Interactions	+	-
+	$U_{C-ELC}+U_{LJ}$	$U_{C-ELC}+U_{HC}$
-	$U_{C-ELC}+U_{HC}$	$U_{C-ELC}+U_{LJ}$

$$\frac{\Delta F(\phi)}{Ak_B T} = \phi \ln \phi + (1 - \phi) \ln(1 - \phi) - \chi \phi^2 + F_{\text{elec}}/(k_B T), \quad (17)$$

where  $A$  represents the two dimensional area of a plane and  $F_{\text{elec}}/(k_B T)$  represents the one loop corrections obtained by integrating the charge density fluctuations.<sup>26</sup>

### III. MODEL AND SIMULATION DETAILS

The model system is composed of a mix of  $N_+$  positively and  $N_-$  negatively charged monomer units in a simulation box of size  $L^3$ . The molecules are confined to a two dimensional plane perpendicular to the  $Z$  axis, with periodic boundary conditions in the  $X$  and  $Y$  directions. Each monomer unit represents a charged biological or polymeric molecule that interacts attractively with a like monomer via hydrophobic forces. In this paper, only symmetric mixtures are considered, where the charge and the radius of the positively and negatively charged monomer units are equivalent. The total system is electroneutral. We are interested in the case where the two dimensional layer exhibits well-defined periodic patterns along the surface of the plane. Fluctuations perpendicular to the monomer plane are restricted.

Constant  $NVT$  molecular dynamics simulations were performed using ESPRESSO, a simulation code developed by the MPIP-Mainz group of Polymer Theory and Simulation (<http://www.espresso.mpg.de>). A stochastic or Langevin thermostat is used to ensure a constant temperature, along with a VERLET algorithm to calculate particle velocities at each time step. The unit of energy is  $\epsilon$ , of length  $\sigma$  and of mass  $m$ . The temperature is then defined in terms of  $\epsilon/k_B T$ , and the time in units of  $\sqrt{\sigma^2 m/\epsilon}$ . A full Coulomb potential is used for calculations of charge-charge interactions. The electrostatic layer correction (ELC) method was developed by Arnold and co-workers to sum the electrostatic energy contribution to the free energy.<sup>28,29</sup> This method is a correction to the P3M Ewald summation technique,<sup>30</sup> in which the Fourier transform of the electrostatic contribution to the energy is summed using a mesh formulation. In addition to full electrostatics, a case of a screened Debye-Hückel interaction is considered to look at the subsequent melting of the periodic structures when the potential is screened. Table I summarizes the interaction potentials between the positive and negative component monomers in the system. The potential between charges is the full Coulomb potential,

$$U_{C-ELC} = \frac{l_B T q_1 q_2}{r}, \quad (18)$$

where  $l_B$  represents the Bjerrum length of the system.

For the present simulation results,  $l_B$ 's of  $0.1\sigma$ ,  $0.2\sigma$ , and  $0.5\sigma$  are considered. Considering an average dielectric per-

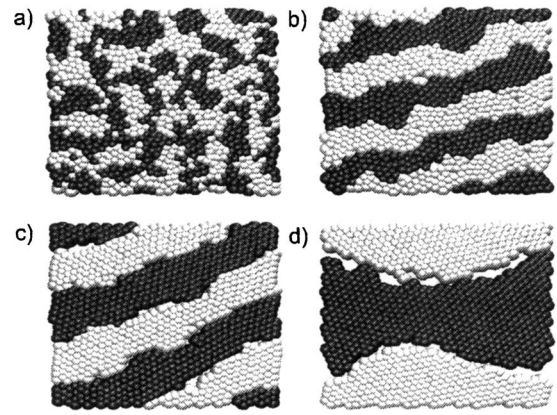


FIG. 1. Snapshots of the system at (a)  $\epsilon=1.0$ , (b) 2.5, and (c)  $4.0k_B T$  at a constant  $l_B$  of  $0.2\sigma$ . Introduction of  $\kappa=20\sigma$  (d) induces a macroscopic phase segregation at  $\epsilon$  of  $4.0k_B T$  and  $l_B$  of  $0.2\sigma$ .

mittivity of the medium ( $\epsilon_r \sim 80$ ) this corresponds to a fairly large head group size ( $\sim 20 \text{ \AA}$ ). The short range interaction between like monomers is the classic Lennard-Jones potential,

$$U_{LJ} = 4\epsilon \left( \left( \frac{\sigma}{r} \right)^{12} - \left( \frac{\sigma}{r} \right)^6 \right), \quad r < r_c, \quad (19)$$

where  $\sigma$  is the monomer radius and the potential is cut at a radius  $r_c$  of  $2.5\sigma$ . An additional term is also added to the potential to keep the derivative continuous at  $r_c$ .  $U_{HC}$  is the same as  $U_{LJ}$  with a cutoff radius  $r_c$  of  $2^{1/6}\sigma$ , including only the repulsive part of the potential, which represents the excluded volume of the molecule.

Initially, a fairly dense surface density  $\rho$  of 0.6 was considered to compare with the phase behavior predicted by the strong segregation theory, while remaining sufficiently far from the two dimensional hard disc crystallization regime of approximately  $\rho=0.89$  determined by previous MC and MD simulations.<sup>31</sup> This also allows a sufficient diffusion for the system to equilibrate.

$$\rho = \frac{(N_+ + N_-) \pi \sigma^2}{4L^2}. \quad (20)$$

Phase behavior in comparison with theory at lower surface densities is slightly more complex and will be discussed in a later paper. The majority of simulation results are presented for a system size of 2000 charged monomers, while finite size effects are explored by increasing the system size by a factor of 2. Approximately  $10^6$  MD steps are used to equilibrate the system; the equilibration time grows increasingly longer at higher values of the Bjerrum length.

### IV. DISCUSSION OF TWO DIMENSIONAL PHASE BEHAVIOR

At lower values of  $\epsilon$ , domains of positive and negative component monomers appear in the system. As the magnitude of  $\epsilon$  increases, the domains begin to increase in size in an isotropic manner, forming a percolated structure. As the value of  $\epsilon$  further increases, the domains begin to elongate and then to orient into a well-defined lamellar, breaking the

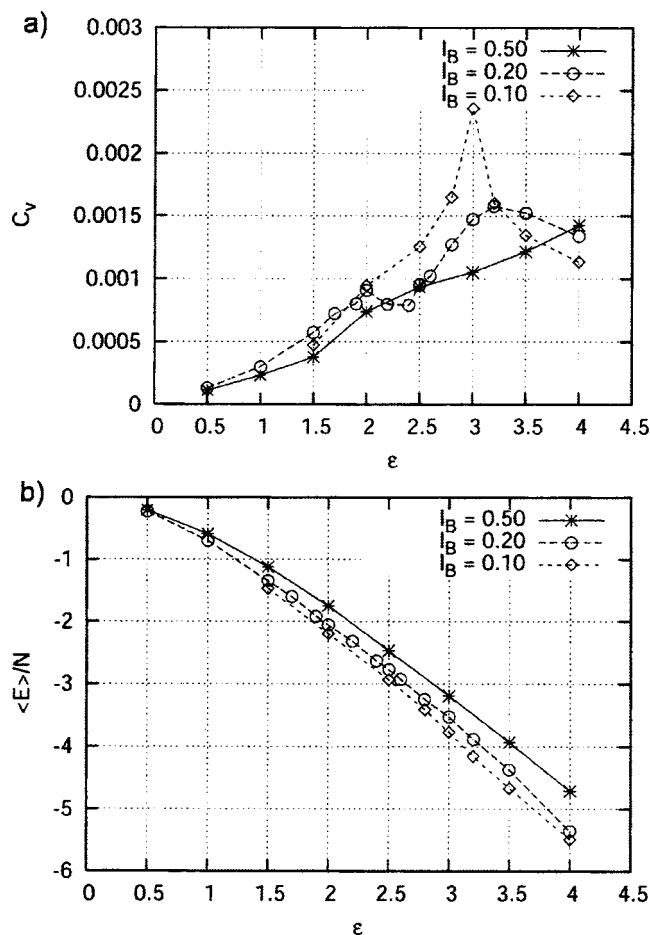


FIG. 2. (a) Heat capacity per particle ( $C_V$ ) and (b) average internal energy ( $\langle E \rangle / N$ ) at several values of the Bjerrum length ( $l_B = 0.1\sigma$ ,  $0.2\sigma$ , and  $0.5\sigma$ ). The heat capacity displays a peak, which corresponds to a crossover from percolated, random domains to a lamellar phase. The magnitude of the peak increases and shifts to the left as the value of the Bjerrum length is decreased.

symmetry of the system. Increasing even further, the lamellar begin to widen, as seen in Fig. 1. The average internal energy and heat capacity per particle are calculated at several values of the Bjerrum length ( $l_B = 0.1\sigma$ ,  $0.2\sigma$ , and  $0.5\sigma$ ). At higher values of  $l_B$ , electrostatics plays a more important role in the equilibrium configuration of the system. The electrostatic repulsion between like charged monomers increases. In order to minimize this contribution to the free energy, the stripes become thinner.

The average internal energy ( $\langle E \rangle / N$ ) and heat capacity per particle ( $C_V$ ) are calculated at two different values of the Bjerrum length ( $l_B = 0.1\sigma$ ,  $0.2\sigma$ , and  $0.5\sigma$ ), as seen in Fig. 2. The average internal energy is less negative at the higher value of  $l_B$  due to the increased repulsion between like charged head groups. At lower values of  $l_B$  the heat capacity displays a peak, which corresponds to the crossover from the percolated phase to the lamellar phase. The magnitude of this peak increases and shifts to the left as the value of the Bjerrum length is decreased.

Lamellar spacing is systematically characterized by the calculation of the two dimensional structure factor  $S(\mathbf{k})$ , where  $\mathbf{r}$  corresponds to a vector in the  $(x, y)$  plane,

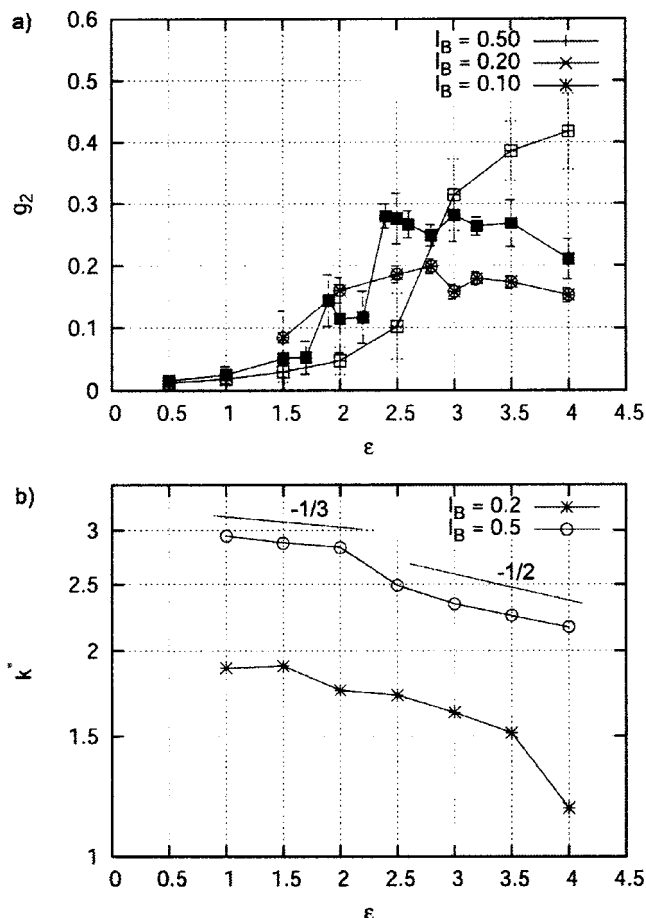


FIG. 3. (a) The interfacial orientational order parameter  $g_2$  at several values of the Bjerrum length ( $l_B = 0.1\sigma$ ,  $0.2\sigma$ , and  $0.5\sigma$ ) as a function of  $\epsilon$ . As the orientational order of the domains increases,  $g_2$  increases from 0 to a finite value. (b) The location of the peak  $k^*$  in the structure factor  $S(\mathbf{k})$  as a function of  $\epsilon$ . The scaling of  $k^*$  with  $\epsilon$  changes from  $-1/3$  to  $-1/2$ .

$$S(\mathbf{k}) = \int g(\mathbf{r} - \mathbf{r}') e^{i\mathbf{k} \cdot \mathbf{r}} e^{i\mathbf{k} \cdot \mathbf{r}'} d^2\mathbf{r}. \quad (21)$$

$S(\mathbf{k})$  displays a peak at  $k^*$  corresponding to the inverse lamellar spacing in the direction perpendicular to the lamellar. As a function of  $\epsilon$ , the peak location corresponds to scaling predictions by the strong segregation theory at high values of  $\epsilon$  ( $k^* \sim \epsilon^{-1/2}$ ), as seen in Fig. 3(b). At lower values, the location is consistent with predictions by the random phase approximation ( $k^* \sim \epsilon^{-1/3}$ ). The orientational order of the domains can be characterized by the interfacial orientational order parameter  $g_2$ ,<sup>32</sup>

$$g_2 = \frac{1}{N} \sum_{i=1}^N \frac{1}{N_i} \sum_{j=1}^{N_i} e^{2i\theta_{ij}}, \quad (22)$$

where  $N_i$  is the number of neighbors of opposite types of monomer at an interface and  $\theta_{ij}$  is the angle between two neighbors. A neighbor is defined as two particles of different types, within the range of the short range attraction ( $r_{ij} < r_c$ ). As the magnitude of the short range attraction increases, the calculated order parameter increases, which corresponds to the ordering of the domains by the development of the orientational order at the interface. The increase in the order of the domains, indicated by an increase in the order

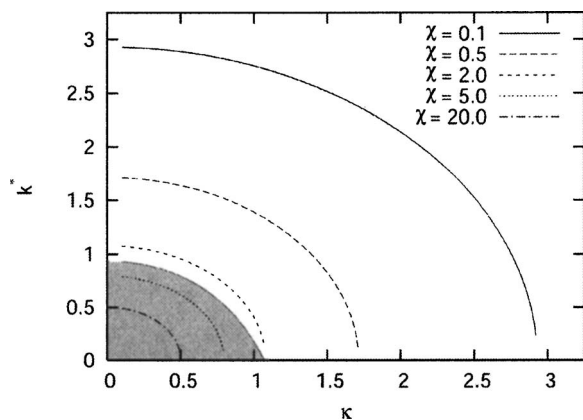


FIG. 4. The location of the peak  $k^*$  in the structure factor  $S(k)$  as a function of  $\kappa$  as predicted by the linear response theory for several values of the short range attraction ( $\chi=0.1, 0.5, 2.0, 5.0,$  and  $20.0$ ) for an intermediate strength of the electrostatics,  $l_B=0.2$ . The shaded area indicates that  $S(k)$  diverges at a finite value of  $k$ .

parameter  $g_2$ , proceeds the location of the peak in the heat capacity. Higher values of the Bjerrum length  $l_B$  correspond to a higher value of the order parameter  $g_2$  for a stronger short range attraction, as seen in Fig. 3(a). As the electrostatic contribution to the segregation increases, the characteristic domain size decreases, but the orientational order of the domains increases. At lower values of  $l_B$ , this initial increase is followed by a leveling off or a slight decrease that corresponds to the formation of holes at the interface. The holes disrupt the orientational order or the hexagonal packing of the monomers within the segregated domains. This is equivalent to the inclusion of a ternary component, with a nonselective interaction between positive and negative components.

Initial examinations on the finite size effects of the system are explored to determine the effect of the periodic boundary conditions on the ordering of the more strongly segregated lamellar. Doubling the size of the system at larger values of the short range attraction ( $\epsilon=4k_B T$ ) quantitatively affects the ordering of the lamellar by decreasing the alignment of the domains along the boundaries of the system and by increasing the fluctuations along the interface. This results in a characteristic decrease in the order parameter  $g_2$  from  $0.43(\pm 0.02)$  to  $0.37(\pm 0.02)$ . Further system sizes were not examined due to the sufficiently high surface density; the calculation of the electrostatic energy is slow to converge at these density ranges.

The introduction of electrostatic screening, or the inclusion of the effects of high salt on the local ordering of the system, is considered by using a screened Debye-Hückel potential instead of the Coulomb potential for electrostatic interactions,

$$U_{C-DH} = \frac{l_B T q_1 q_2 e^{-\kappa r}}{r}, \quad (23)$$

where  $\kappa$  represents the screening length due to the surrounding three dimensional solution of ions.

At higher values of electrostatic screening ( $\kappa=5\sigma, 10\sigma,$  and  $15\sigma$ ), examining the behavior of the system with an intermediate value of the short range attraction ( $\epsilon=2.0$ ), the

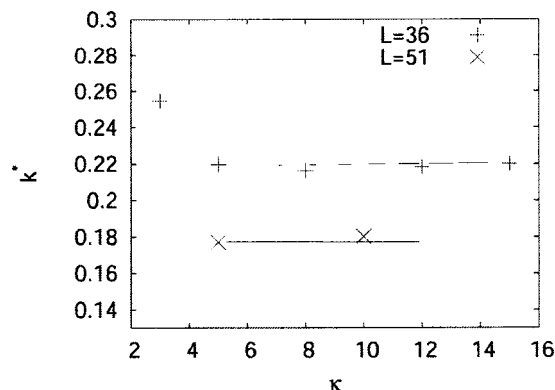


FIG. 5. The location of the peak  $k^*$  in the structure factor  $S(k)$  as a function of  $\kappa$  from simulation results spanning a range of the screening parameter ( $\kappa=3-15\sigma$ ) at an intermediate value of the short range attraction ( $\epsilon=2.0$ ). Increasing the size of the system from  $L=36$  to  $L=51$  decreases the average value of  $k^*$ .

system phase segregates into two macroscopic charged domains of positive and negative ions. The peak in the structure factor indicates that the segregation length scale is nearly constant as a function of the screening length. This is in agreement with the analytic theory.<sup>17</sup> The location of the peak shifts to lower values with an increase in the characteristic size of the simulation box. To determine if these simulation results are consistent with theoretical predictions, we examine the behavior of the inverse structure factor [Eq. (16)] in a regime where the scaling of the peak in the structure factor from simulation results is still consistent with the linear response theory. We find that as  $\kappa$ , the magnitude of screening by the ions of solution, increases, the value of  $q^*$  goes continuously to zero, as seen in Fig. 4,

$$q^* = \left( -\kappa^2 + \left( \frac{4\pi l_B}{\chi} \right)^{2/3} \right)^{1/2}, \quad (24)$$

before the structure factor diverges, at which there is a macroscopic phase segregation. At higher values of the short range attraction, the structure factor diverges when  $q^* > 0$ . This is in agreement with analytical predictions from the strong segregation regime, which predicts a discontinuous jump from finite sized periodic cells to an infinite cell at a value of  $\kappa$  which is inversely proportional to the periodic length scale of the system,<sup>17</sup> as shown in Fig. 5.

## V. CONCLUSIONS

Molecular dynamics simulations of oppositely charged monomers, interacting with a short range LJ potential and confined to a two dimensional plane, are examined at different strengths of the short range attraction and the long range electrostatics. The system exhibits well-defined domains; the width and ordering of the domains are dependent on the depth of the LJ well,  $\epsilon$ , and the strength of the Coulomb interactions,  $l_B$ . The length scale of the ordering of the system can be quantitatively characterized by the two dimensional Fourier transform of the density,  $S(\mathbf{k})$ , where  $\mathbf{k}$  is the inverse spacing of the system.  $S(\mathbf{k})$  has a peak  $k^*$  which scales with the line tension of the domains,  $\gamma$ . The underlying assumption of the strong segregation theory is that the

microphase regions of charge are well defined and periodic, with a line tension  $\gamma$  that is proportional to  $\chi$ . Since the magnitude of the short range attraction  $\epsilon$  is proportional the Flory-Huggins interaction parameter  $\chi$ ,  $k^*$  should scale with  $\epsilon$  in the regimes where the strong segregation theory holds.<sup>17</sup> It is shown that, at higher values of  $\epsilon$ , the scaling of  $k^*$  with  $\epsilon$  is consistent with theory. At lower values of  $\epsilon$ , a different scaling is found, which is consistent with that which is found using the linear response theory. Electrostatics represents a more important contribution to the characterization of the interfacial line tension in this regime.

The degree of ordering can be examined by the calculation of the interfacial orientational order parameter  $g_2$ . The transition from a random, percolated domain structure to a well-defined lamellar is a gradual transition that is demonstrated by the gradual increase of the parameter  $g_2$  as a function of  $\epsilon$ . This result is consistent with what one would exhibit with a Kosterlitz-Thouless-type transition,<sup>31</sup> in which the two dimensional ordering of the system exhibits a continuous phase transition that can be defined by a similar positional order parameter. Initial examinations of the finite size effects of the system indicate that the degree of ordering is slightly influenced by the periodicity of the simulation box; however, further examinations were not made due to the computational intensiveness of the electrostatic energy term. Decreasing the strength of the electrostatics in the system by changing the charged interaction from a straight Coulomb potential to a screened Debye-Hückel interaction, the ordering of the system disappears and the mixture phase segregates. This is consistent with analytical arguments.

## ACKNOWLEDGMENTS

This work was supported by the IGERT-NSF Fellowship awarded to one of the authors (S.L.) and by the NSF Grant Nos. DMR-0414446 and DMR-0503943. S.L. would like to acknowledge the group of Christian Holm, who is now at the Frankfurt Institute for Advanced Studies, Johann Wolfgang Goethe-Universität, including Axel Arnold and Bernward Mann for scientific and simulation discussions.

- <sup>1</sup>E. Raspaud, I. Chaperon, A. Leforestier, and F. Livolant, *Biophys. J.* **77**, 1547 (1999).
- <sup>2</sup>L. K. Sanders, C. Guáqueta, T. E. Angelini, J. W. Lee, S. C. Slimmer, E. Luijten, and G. C. L. Wong, *Phys. Rev. Lett.* **95**, 108302 (2005).
- <sup>3</sup>M. Dubois, B. Deme, T. Gulik-Krzywicki, J. C. Debieu, C. Vautrin, E. Perez, and T. Zemb, *Nature (London)* **411**, 672 (2001).
- <sup>4</sup>M. Biesalski, R. Tu, and M. V. Tirrell, *Langmuir* **21**, 5663 (2005).
- <sup>5</sup>E. Kaler, K. Herrington, and A. Murthy, *J. Phys. Chem.* **96**, 6698 (1992).
- <sup>6</sup>D. C. Pozzo and L. M. Walker, *Macromol. Symp.* **227**, 203 (2005).
- <sup>7</sup>J. D. Hartgerink, E. Beniash, and S. I. Stupp, *Science* **294**, 1684 (2001).
- <sup>8</sup>J. Liu, S. Qi, J. T. Groves, and A. K. Chakraborty, *J. Phys. Chem. B* **109**, 19960 (2005).
- <sup>9</sup>J. Widom and R. L. Baldwin, *J. Mol. Biol.* **144**, 431 (1980).
- <sup>10</sup>E. Raspaud, M. Olvera de la Cruz, J. L. Sikorav, and F. Livolant, *Biophys. J.* **74**, 381 (1998).
- <sup>11</sup>M. Olvera de la Cruz, L. Belloni, M. Delsanti, J. P. Dalbiez, O. Spalla, and M. Drifford, *J. Chem. Phys.* **103**, 5781 (1995).
- <sup>12</sup>Y. Levin, *Rep. Prog. Phys.* **65**, 1577 (2002).
- <sup>13</sup>F. J. Solis and M. Olvera de la Cruz, *J. Chem. Phys.* **112**, 2030 (2000).
- <sup>14</sup>S. Liu and M. Muthukumar, *J. Chem. Phys.* **116**, 9975 (2002).
- <sup>15</sup>J. F. Liu and W. A. Ducker, *J. Phys. Chem. B* **103**, 8558 (1999).
- <sup>16</sup>E. E. Meyer, Q. Lin, T. Hassenkam, E. Oroudjev, and J. N. Israelachvili, *PRAN*, **102**, 6834 (2005).
- <sup>17</sup>F. J. Solis, S. I. Stupp, and M. Olvera de la Cruz, *J. Chem. Phys.* **122**, 054905 (2005).
- <sup>18</sup>Y. S. Velichko and M. Olvera de la Cruz, *Phys. Rev. E* **72**, 041920 (2005).
- <sup>19</sup>U. Loew, V. J. Emery, K. Fabricius, and S. A. Kivelson, *Phys. Rev. Lett.* **72**, 1918 (1994).
- <sup>20</sup>L. Leibler, *Macromolecules* **13**, 1602 (1980).
- <sup>21</sup>M. D. Lefebvre, M. Olvera de la Cruz, and K. R. Shull, *Macromolecules* **37**, 1118 (2004).
- <sup>22</sup>P. M. Chaikin and T. C. Lubensky, *Principles of Condensed Matter Physics* (Cambridge University Press, Cambridge, England, 1995).
- <sup>23</sup>E. W. Kaler, K. L. Herrington, A. K. Murthy, and J. A. N. Zasadzinski, *J. Chem. Phys.* **96**, 6698 (1992).
- <sup>24</sup>I. I. Potemkin, E. Yu. Kramarenko, A. R. Kholklov, R. G. Winkler, P. Reneker, P. Eibek, J. P. Spatz, and M. Moeller, *Langmuir* **15**, 7290 (1999).
- <sup>25</sup>P. Gonzalez-Mozuelos and M. Olvera de la Cruz, *J. Chem. Phys.* **100**, 507 (1994).
- <sup>26</sup>B. Y. Borue and I. Y. Erukhimovich, *Macromolecules* **21**, 3240 (1988).
- <sup>27</sup>S. Prestipino, F. Saija, and P. V. Giaquinta, *Phys. Rev. E* **71**, 050102 (2005).
- <sup>28</sup>A. Arnold, J. Joannis, and C. Holm, *J. Chem. Phys.* **117**, 2496 (2002).
- <sup>29</sup>J. Joannis, A. Arnold, and C. Holm, *J. Chem. Phys.* **117**, 2503 (2002).
- <sup>30</sup>R. W. Hockney and J. W. Eastwood, *Computer Simulation Using Particles* (Hilger, London, 1988).
- <sup>31</sup>A. Jaster, *Phys. Rev. E* **59**, 2594 (1999).
- <sup>32</sup>A. D. Stoycheva and S. J. Singer, *Phys. Rev. Lett.* **84**, 4657 (2000).